Evolutionary Optimization of a Motorcycle Traction Control System Based on Fuzzy Logic

Article *in* IEEE Transactions on Fuzzy Systems · October 2015

DOI: 10.1109/TFUZZ.2014.2370681

CITATIONS
21

READS
338

4 authors, including:

Juan Cabrera
University of Malaga
69 PUBLICATIONS **940** CITATIONS
SEE PROFILE

Juan Castillo
University of Malaga
36 PUBLICATIONS **423** CITATIONS
SEE PROFILE

Antonio Ortiz
University of Malaga
32 PUBLICATIONS **366** CITATIONS
SEE PROFILE

Evolutionary Optimization of a Motorcycle Traction Control System Based on Fuzzy Logic

Cabrera J.A., Castillo J.J., Carabias E. and Ortiz A.

***Abstract*— Braking and traction control systems are fundamental vehicle safety equipments. The first ones prevent the wheels from locking, maintaining, when possible, the handling of the vehicle under emergency braking. While the second ones control wheel slip when excessive torque is applied on driving wheels. The aim of this work is to develop and implement a new control model of a traction control system to be installed on a motorcycle, regulating the slip in traction and improving dynamic behavior of two-wheeled vehicles. This paper presents a novel traction control algorithm which makes use of a fuzzy logic control block. Two strategies to create the control block have been carried out. In the first one, the parameters that define the fuzzy logic controller have been tuned according to experience. In the second one, the parameters have been obtained by means of an Evolutionary Algorithm (EA) in order to design an augmented traction controller. It has been proved that the use of EA can improve the fuzzy logic based control algorithm, obtaining better results than those produced with the control tuned only by experience.**

***Index Terms*— Evolutionary computation, fuzzy control, traction control system, vehicle safety.**

I. Introduction

THE appearance of anti-lock braking systems (ABS) and traction control systems (TCS) have been some of the most major developments in vehicle safety. These systems have been evolving since their origin, always keeping the same objective, but using increasingly sophisticated algorithms and complex brake and torque control architectures. It has also become gradually common to find systems that work in conjunction with other safety features.

These systems began to be installed in four-wheeled vehicles, being much more complex to develop them for two-wheeled vehicles. However, there is a strong interest in the development and implementation of these systems in motorcycles, especially to improve active safety in these vehicles as recognized in [1]. Although anti-lock braking systems are extensively used in two-wheeled vehicles, few attempts have been developed in traction control systems for motorcycles. For example, in [2], a traction control system for a ride-by-wire sport motorcycle is proposed. A second-order sliding mode control is suggested. The controller uses the position of the electronic throttle as the control variable. In [3], a low-cost traction control for motocross and supermotard motorcycles is described. Control is performed using the difference in speed between front and rear wheels and the torque is controlled introducing cuts in the ignition spark. Similarly, a traction control system using fuzzy sliding mode control is proposed in [4] for an electric scooter with a direct-driven wheel motor. Another work discusses the motorcycle engine-to-slip dynamics to be used in traction control designs, [5]. Finally, a complete scheme of relationships between elements and parameters involved in traction control systems is shown in [6].

On the other hand, several studies on braking control systems for two-wheeled vehicles have been developed. In [7], a linear parameter-varying slip control for two-wheeled vehicles equipped with electromechanical front wheel brakes is studied. An antilock brake system for lightweight motorcycles using a single channel actuator was developed in [8]. Finally, a premature work on ABS systems for motorcycles was carried out in [9].

An essential part of TCS and ABS systems is the control algorithm. The study of new algorithms is of great interest to research groups in vehicle dynamics, existing a big number of papers focused on this topic. Due to the absolute secrecy of commercial equipment manufacturers, control algorithms behave, from the user's point of view, as a "black box", which takes the angular velocity of each wheel and other measures as inputs for the stability and traction control, having the necessary action as output. At present, control model developments are mainly based on techniques that allow an adaptable control in the different conditions in which the motorbike rider has to perform braking or accelerating maneuvers.

The main problem of these systems is to determine the slip (s) and friction coefficient (μ), which occur in the wheels to operate within the optimal tire-road friction curve (Fig. 1) and thus obtain the appropriate behavior in the braking and

This paragraph of the first footnote will contain the date on which you submitted your paper for review. This work was supported in part by the Spanish Innovation Science Ministry under Grant TRA2011-23261

J.A. Cabrera is with the Mechanical Engineering Departament, University of Málaga, c/ Doctor Ortiz Ramos s/n 29071 Málaga (SPAIN) (phone: 34-951952371; fax: 34-951952605; e-mail: jcabrera@ uma.es).

J.J. Castillo is with the Mechanical Engineering Departament, University of Málaga, c/ Doctor Ortiz Ramos s/n 29071 Málaga (SPAIN) (phone: 34-951952372; fax: 34-951952605; e-mail: juancas@ uma.es).

E. Carabias is with the Mechanical Engineering Departament, University of Málaga, c/ Doctor Ortiz Ramos s/n 29071 Málaga (SPAIN) (phone: 34-951952381; fax: 34-951952605; e-mail: eca@ uma.es).

A. Ortiz is with the Mechanical Engineering Departament, University of Málaga, c/ Doctor Ortiz Ramos s/n 29071 Málaga (SPAIN) (phone: 34-951952367; fax: 34-951952605; e-mail: aortizf@ uma.es).

traction process and cornering stability of a motorcycle. The curves that relate the friction coefficient and the slip in traction or braking processes are similar, (Fig. 1). The purpose of TCS and ABS systems is to maintain the slip ratio within the optimal control zone as much as possible, which is characterized by the maximum allowable friction coefficient as we can see in Fig. 1. When the slip ratio exceeds the slip that produces the maximum friction coefficient, the longitudinal and lateral tire forces decrease drastically. One of the obstacles in the development of robust TCS and ABS systems has traditionally been the real-time estimation of the wheel-slip versus adhesion-coefficient characteristics for different tire types and road surface conditions [10-12].

The difference between a TCS and ABS lies in the dynamics of the control process. The first one uses the braking torque as control variable while the second one uses the traction torque. Some TCS can also use the rear braking and traction torque to enhance the response time of the system. In this paper we will focus on TCS, since the dynamics of the control variables are different from ABS and have been less studied in bibliography.

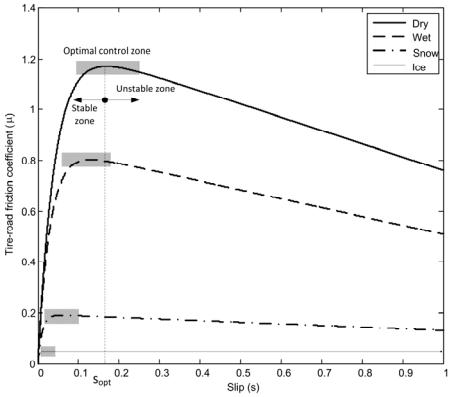

Fig. 1. Friction coefficient curves.

After the required dynamics parameters have been obtained, another important aspect in motorcycle TCS systems is to perform a control on the torque applied on the rear wheel to maintain rear tire force in the maximum value. Among the new control techniques in the traction process, control techniques based on sliding control [2] and on fuzzy logic [3][4] should be noted.

There are many works related to braking and traction fuzzy control in vehicles. The use of fuzzy logic in vehicle systems is highly successful due to its easy development and control robustness [11-14]. In fact, in [15], fuzzy logic is considered as one of the possibilities to improve traction control systems. The objective of this work is to optimize the membership function of the linguistic variables and the if-then rules in a fuzzy logic traction control. The optimization process will be carried out by means of a genetic algorithm and the obtained results will be compared with the traction control previously developed by experience.

It should be noted that several researches have used evolutionary techniques to optimize a fuzzy control. The difficulty of using genetic algorithms in fuzzy block optimization lies in the application of genetic operators to membership functions. The crossover and mutation processes of membership functions can give rise to many invalid individuals. Normally, restrictions on the evolution process are imposed to overcome this problem, which limits the search capability of the algorithms. For example, in [16] current framework and new trends in genetic fuzzy systems are pointed out. They show that, currently, there is an increasing interest to augment fuzzy systems with learning and adaptation capabilities. Evolutionary algorithms are one of the most successful approaches to obtain fuzzy systems with these kinds of qualities. In [17] a genetic algorithm is used to learn logic rules and membership functions in a fuzzy logic controller. The obtained controller is validated with a theoretical car-following model. An innovative evolutionary technique called differential evolution (DE) is used for the automatic design of a hierarchical fuzzy logic control in [18].

Overall, the previously proposed methods optimize rules and membership functions by applying certain restrictions on the latter. This paper presents a new fuzzy optimization method that optimizes both membership functions and rules with almost no restriction in the search space.

Hence, a new fuzzy traction control system is developed in this paper using an evolutionary algorithm to optimize it. All the components of the new control model are presented in Section 2. A fuzzy logic control block based on experience is developed in Section 3. Section 4 presents the control system optimized by genetic algorithms. In Section 5 simulation results are included. Finally, conclusions are drawn in Section 6.

II. Control Model By Fuzzy Logic

One of the most influential variables in motorcycle traction processes is the longitudinal force of the rear wheel, $F_{x,r}$. The longitudinal force should be as large as possible to achieve maximum accelerations. This force is proportional to the vertical load on the rear wheel, N_r. The proportionality term is called the friction coefficient and is denoted by μ_x.

$$F_{x,r} = \mu_x N_r \tag{1}$$

Under high acceleration, the tire increases slippage between wheel and road. This phenomenon is measured by a parameter called longitudinal slip, s.

$$s = 1 - \frac{v_x}{\omega_r R_r} \tag{2}$$

Being v_x the longitudinal velocity of the motorcycle, ω_r the angular velocity of the rear wheel and R_r the rear tire radius.

The road friction coefficient (μ_x) depends on the slip and the surface (Fig. 1). The control has to keep the slip in the area in which the adhesion coefficient is the highest for any surface as much as possible. There are several equations to express the relationship between the friction coefficient and the slip for different road surface conditions, speeds, pressures, etc., such as the "Magic Formula" by Pacejka [19] and the Burckhardt model [20], as shown in Fig. 1.

In Fig. 2 a block diagram shows the relationship between the elements that have been developed for the proposed

traction control system. This paper is focused on the control block (Fig. 2 (4)), where the regulation is performed. However, a brief explanation of the performance of the parameter estimation and optimal slip estimation blocks is included.

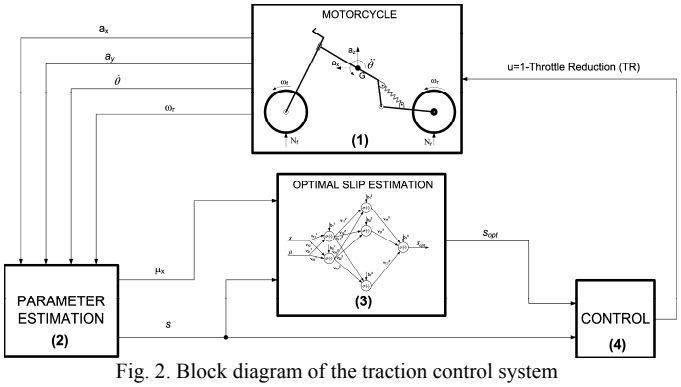

Fig. 2. Block diagram of the traction control system

For this work, the longitudinal and vertical acceleration (a_x, a_z), pitch rate ($\dot{\theta}$) and rear wheel angular velocity (ω_r) of the motorcycle are measurements in our traction control system. These variables are used to obtain the slip and friction coefficient using an extended Kalman filter (EKF). The parameter estimation algorithm makes use of a three-degree-of-freedom longitudinal-vertical motorcycle model to simulate the vehicle when moving in a straight line (Fig. 3).

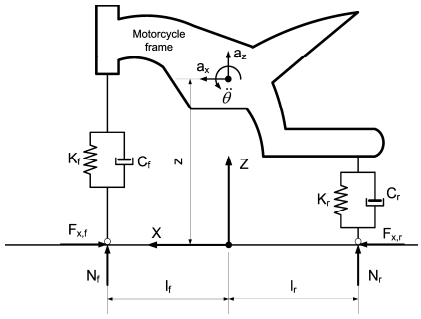

Fig. 3. Motorcycle model.

The model used for the estimates is derived from rigid body dynamics equations. These equations are:

$$Ma_x = M\left(\ddot{x} + \dot{\theta}v_z\right) = F_{x,r} - Cv_x^2 - F_{x,f} \tag{3}$$

$$Ma_z = M\left(\ddot{z} - \dot{\theta}v_x + g\right) = N_f + N_r \tag{4}$$

$$I_y\ddot{\theta} = N_r l_r - N_f l_f - \left(F_{x,r} - F_{x,f}\right)z \tag{5}$$

Where M is the mass of the motorcycle, a_x and v_x are the longitudinal acceleration and velocity respectively, a_z, v_z and z are the vertical acceleration, velocity and displacement, $\ddot{\theta}$ and $\dot{\theta}$ are the pitch acceleration and rate. $F_{x,r}$ is the longitudinal force on the rear wheel (equation 1), $F_{x,f}$ is the rolling resistance force and C is the aerodynamic drag coefficient. N_f and N_r are the vertical load on the front and rear wheel respectively, I_y is the moment of inertia about the pitch axis that passes through the mass center. Finally, l_f and l_r are the front and rear half-length. The rolling resistance force has been considered as follows:

$$F_{x,f} = (C_1 + C_2{v_x}^2)N_f \tag{6}$$

Where C_1 and C_2 are constants.

An EKF (Extended Kalman Filter) based parameter estimation block is used to obtain the longitudinal velocity estimate and other parameters necessary to determine the slip and tire-road friction coefficient. The EKF assumes the following system.

$$x_k = f_{k-1}(x_{k-1}) + w_{k-1} \tag{7}$$

$$j_k = h_k(x_k) + v_k \tag{8}$$

Where w_k and v_k variables represent the noise in the model and observations respectively, x_k is the state variables vector and j_k is the measurement vector.

It is necessary to use dynamic equations of our state variables and equations that relate the measures with the variables to perform the estimation. The state variables vector is $x(k) = \left[F_{x,r}, N_r, N_f, v_x\right]^T$ and the measurement vector is $j(k) = \left[a_x, a_z, \ddot{\theta}\right]^T$. A dynamic model known as first order *"random walk"* has been used to estimate forces $F_{x,r}$, N_r, and N_f. [21]. A finite difference equation of longitudinal dynamics of the motorcycle has been used to estimate the longitudinal velocity of the motorcycle, v_x. Therefore, the dynamic equations of the state vector variables are as follows:

$$x(k) = \begin{bmatrix} F_{x,r}(k) \\ N_r(k) \\ N_f(k) \\ v_x(k) \end{bmatrix} = f_{k-1}(x_{k-1})$$

$$= \begin{bmatrix} F_{x,r}(k-1) \\ N_r(k-1) \\ N_f(k-1) \\ v_x(k-1) + \Delta t\left(\frac{F_{x,r}(k-1) - Cv_x^2(k-1) - \left(C_1 + C_2{v_x}^2(k-1)\right)N_f(k-1)}{M} - \dot{\theta}v_z\right) \end{bmatrix} \tag{9}$$

Discrete model equations relate the measures with the state variables vector.

$$j(k) = \begin{bmatrix} a_x(k) \\ a_z(k) \\ \ddot{\theta}(k) \end{bmatrix} = h_k(x_k)$$

$$= \begin{bmatrix} \frac{F_{x,r}(k) - Cv_x^2(k) - \left(C_1 + C_2{v_x}^2(k)\right)N_f(k)}{M} \\ \frac{N_f(k) + N_r(k) - Mg}{M} \\ \frac{N_r(k)l_r - N_f(k)l_f - \left(F_{x,r}(k) - \left(C_1 + C_2{v_x}^2(k)\right)N_f(k)\right)z(k)}{I_y} \end{bmatrix} \tag{10}$$

Therefore, the EKF algorithm estimates vertical forces, longitudinal force and speed. With these estimated values we can obtain the slip and friction coefficient at each time step.

$$s_{k,est} = 1 - \frac{v_k(k)}{w_r(k).R_r} \tag{11}$$

$$\mu_{k,est} = \frac{F_{x,r}(k)}{N_r(k)} \tag{12}$$

Once we have estimated the slip (s) and friction coefficient (μ_x) a fuzzy-neural network block is used to obtain the optimal slip (s_{opt}), i.e., the slip where the friction coefficient is the highest for that surface (see Fig. 1). This stage is included in block number 3 in Fig. 2.

For this purpose, a first stage is used to calculate the road type. In this stage we use a fuzzy logic identification block. This block is broadly explained in [11]. Next, the output of the fuzzy logic identification block is used to obtain the optimal slip (s_{opt}). The neural network that we proposed is composed of three layers. Activation functions for the first two layers are of the "Symmetric Sigmoid" type, being the "Linear" type for the last layer. The neural network inputs are: road type, adhesion coefficient (μ) and slip (s), and the output is a number that indicates optimum slip (s_{opt}) of the road the motorcycle is circulating on. To know appropriate weights and bias, the neural network training is carried out. This will take a series of road type, adhesion coefficient and slip values of which the optimal slip is known. The weights and biases are adjusted from these input values.

Therefore, the inputs to our proposed control block are the estimated slip (s) and optimal slip (s_{opt}) and the output is the throttle reduction (TR).

The goal of this work is to develop this fuzzy control block by means of experience and to compare it with an augmented controller to improve the performance of the proposed TCS. Control techniques based on fuzzy logic are used to control non-linear systems.

Fuzzy logic processes are relatively easy to implement, so the use of this technique has extended increasingly. Furthermore, the operation to control a process is similar to human intuition and it allows introducing the knowledge of an expert. We have to take into account that the process we are working on is non-linear and very complex. This is due to the fact that the traction control system performs a rear wheel torque or a throttle reduction and, consequently, a slip reduction. However, even when complex models are available, they do not include all the factors that influence in the relationship between actuation and slip change, so we have to base on knowledge.

Our fuzzy control will be a block (Fig. 4), whose inputs are the difference between the slip and the optimal slip (*error*) and how the error is modified (*derror*). The output of the block is a value between 0 and 1 that corresponds to the throttle reduction (TR), although, the actuation in the motorcycle is: u(t)=1-TR(t) (Fig. 2), i.e, when the output of the fuzzy control block is 0, then the motorcycle throttle is full and zero when the output of the fuzzy control block is 1, so the control system can accelerate or decelerate depending on throttle reduction.

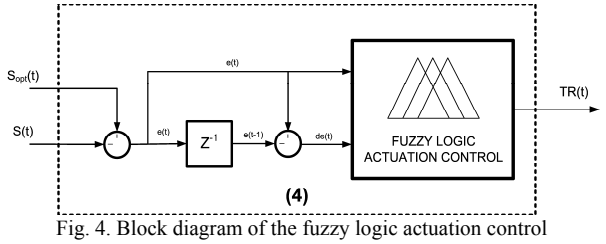

Fig. 4. Block diagram of the fuzzy logic actuation control

To the proposed control system the input parameters are shown in the following equations, being s the estimated slip and s_{opt} the optimal slip.

$$e(t) = s_{opt}(t) - s(t) \tag{13}$$

$$de(t) = e(t) - e(t - T) \tag{14}$$

Equation (13) determines the error between the optimal slip, obtained from the type of road, and the estimated slip. The error is used to know if the system is in the stable or unstable zone and how far the control is from the optimum. Equation (14) defines the error difference, the difference between the error and the error in the previous instant. The error difference variable points out the dynamics of the system. The error range varies between [-1;1], given the fact that the slip varies between [0;1] and therefore the error difference will be between [-2;2]. Actually, if it is taken into account that the optimal slip is less than 0.2 (Fig. 1), the error range is [-1;0.2]. The range of the error difference can be reduced, according to experience, to [-0.4;0.4]. The system output will be a value between 0 and 1, being 0 when actuation is not necessary (zero percent of throttle reduction, that is, the motorcycle continues pulling the throttle) and 1 the maximum actuation (hundred percent throttle reduction, that is, the control turns the gas off).

Once the input and output variables have been defined, we must consider that the traction control system does not have to operate all the time. The TCS will have to actuate only when the difference between the front and the rear wheel velocity is higher than a predefined value.

III. Control Based On Experience

In this section we describe a fuzzy logic controller to be used in the TCS tuned by experience. The membership functions are based on the knowledge of an expert operator, which is our knowledge of how an actuation produces variations in the slip. The membership functions for the established parameters are shown in Fig. 5. As we can observe, the membership functions are triangular and trapezoidal. The values for each of the variables are reflected in Table I.

TABLE I
Membership Function Values. (a) Error Values. (b) Difference Error Values. (c) Actuation Values

error	
ELN	Extra large negative error
LN	Large negative error
N	Negative error
ZE	Zero error
P	Positive error

a)

Difference error	
LN	Large negative difference error
N	Negative difference error
ZE	Zero difference error
P	Positive difference error
LP	Large positive difference error

b)

Actuation	
ZP	Zero actuation
SSP	Smaller small actuation
SP	Small actuation
MP	Medium actuation
LP	Large actuation
ELP	Extra large actuation

c)

In our inference system, rules only have an and-operator, which is defined in [22] and the centroid method has been used in the defuzzification phase [22-23].

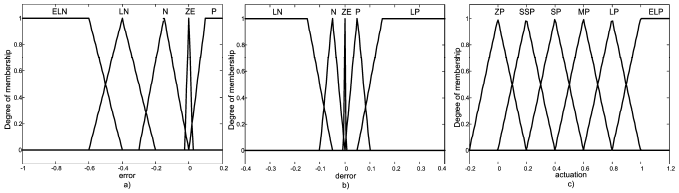

Fig. 5. Based on experience membership functions. (a) Error input. (b) Derror input. (c) Actuation output

It should be noted that the membership functions for the

error input variable are not symmetrical with regards to the Y-axis. This is due to the fact that the optimal slip does not reach a value of more than 0.05-0.2, so, according to equation (13), the difference between the optimal slip, $s_{opt}(t)$, and the slip in that instant, $s(t)$, can only vary from approximately -0.2 to 0.85. Therefore the negative values of the error will be higher than the positive ones. However, the difference error membership functions are symmetric because its range is symmetric. Finally, it is observed that the zero actuation membership functions can take values of less than zero, which is due to how we are using the centroid method. Therefore, there is a combination of inputs whose center of gravity is zero and the output can take a zero value. Something similar happens to the maximum actuation.

Once the input and output variables have been established, a study of the behaviour required for the control is carried out to define the rules that govern it. To establish the control rules, six differentiated cases of behaviour of the input variables are established (see Fig. 6).

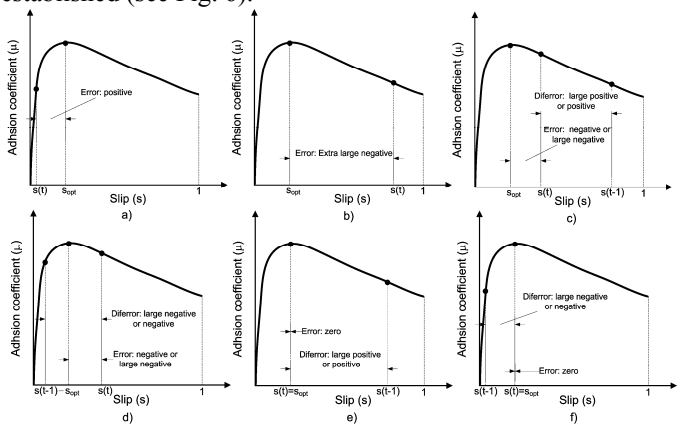

Fig. 6. Error and error difference behavior. (a) Positive error. (b) Extra large negative error. (c) Negative error and Positive error difference. (d) Negative error and negative error difference. (e) Zero error and positive error difference. (f) Zero error and negative error difference

In the first case, as one can observe in Fig. 6a, the error is positive, and the actuation will be zero (no variation of the throttle position) because we are in the part of the curve where we have not reached the optimal slip coefficient. In the second case (Fig. 6b), the error is extra large negative, which means that the wheel is skidding or about to skid so we have to carry out a very high actuation or throttle reduction. These are the two simplest cases to establish the rules. For the following rules we have to take the difference of the committed error into consideration. These rules define the behavior when we are near the optimal slip, that is, when the error is zero or when the optimal slip has been slightly exceeded.

First we will establish the rules when the error is negative or large negative. In other words we have exceeded the limit of the optimal slip. To establish the rules, we will observe Fig. 6c-6d.

In Fig. 6c the error is negative or large negative and the difference error is positive. In this case, the error was bigger in the previous instant than the existing error in this instant of time. This means that we come from a situation of high reduction of the throttle position and we are reducing the slip, which means that we should change to a lower percentage of throttle reduction depending on whether the error is large negative o negative. In case the slip in the previous instant is the same as in this instant, that is, the error difference is zero, we will maintain a very high percentage of throttle reduction. This is because we need to decrease the slip faster.

Fig. 6d shows the case in which the error continues being large negative or negative and the error difference is negative too. In this case, in the previous instant we were in the zone where we did not exceed the optimal slip or we exceeded it but less than in the current instant, so we apply zero throttle reduction, which means that if we have exceeded the optimal slip more in the current time, we have to increase the throttle reduction.

Following, we will establish the rules for the case in which the committed error is zero, that is, when the slip in that instant of time is equal to the optimal slip. This is shown in Fig. 6e-6f.

In the first case, when the error is zero and the slip in the previous instant was superior to the optimal slip (Fig. 6e), that is, the error difference was positive, then the same thing happens as in the previous case shown in Fig. 6c . In other words, we were in a situation in which the throttle reduction was high and we have managed to reduce the slip, so we will change to a lower percentage of throttle reduction, but with a value which is smaller than in the negative error case. In case the slip in the previous instant was also the optimal slip, then we will maintain zero percent throttle reduction.

Finally, when the error is zero and the slip in the previous instant was inferior to the slip limit, (Fig. 6f) it means that we were in a situation in which the throttle reduction was zero and we managed to increase the slip, so the throttle reduction has to be increased to avoid system instability.

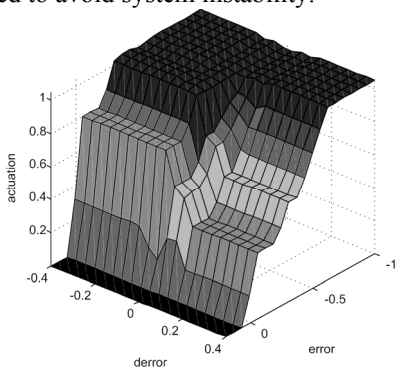

Fig. 7.- Actuation surface

TABLE II
FUZZY CONTROL RULES

error \ diferror	LN	N	ZE	P	LP
ELN	ELP	ELP	ELP	ELP	ELP
LN	ELP	ELP	ELP	LP	MP
N	LP	LP	LP	MP	SP
ZE	SP	SSP	ZP	SP	SSP
P	ZP	ZP	ZP	ZP	ZP

Once the different states have been explained, the rules of the based-on-experience fuzzy controller can be established

(see Table II). The surface that the inference system generates is shown next (see Fig. 7).

The performance of this control is verified by simulations, but the stability is not theoretically guaranteed. A robustness and stability evaluation has been included in appendix A.

IV. Control Based On Optimization

As we have seen in the previous section, the development of a fuzzy control based on experience requires huge knowledge of the process that we need to control and we have to carry out simulations and tests to improve and fit control performance. Major decisions have to be made concerning determination of the input and output variables, the input and output space partition, the shape of membership functions, and the reasoning method. Evolutionary algorithms can realize this task automatically although they cannot assure that the found solution will be optimal. However, this solution can satisfy the user's needs without demanding a great awareness of the problem. In this section, a fuzzy logic block, whose functions and rules have been optimized by evolutionary algorithms, is presented.

In this work, we propose an optimization method that optimizes rules and membership functions. The fuzzy block is defined by the membership functions for each input and output variables and for the reasoning method (rules and their weights). In our case, the membership functions for the error and difference error input variables are five triangular functions and six triangular functions for the actuation output variable. The rules came up when we combined the five functions of the input variables. Rules with only one antecedent are not allowed, so we have 25 rules. The consequent of each rule is a function of the output variable.

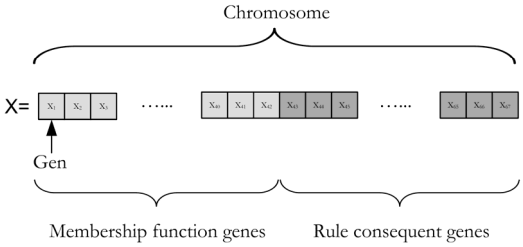

Fig. 8. Chromosome

Hence, the complete number of parameters to optimize is 67. To define the membership functions and rules we need 42 and 25 parameters respectively. Due to this, the chromosome is divided in two differentiated sections as seen in Fig. 8. The first section collects the representative values which define the membership functions. These values are real numbers. The second one reproduces the consequent of the rules. Therefore, each gene of this section is an integer number between [0,6], where 0 represents the exclusion of the rules and other numbers indicate the inclusion of the rules with one of the six membership functions of the output variable.

The scheme of the optimization algorithm is shown in Fig. 9. The first step in the algorithm is the random generation of the initial population. As we pointed out above, the chromosome or individual of the population consists of 67 genes. The first 42 genes correspond to the definitions of membership functions (see Fig. 8). The error and difference error variables are made up by five triangular membership functions and the actuation variables by six. Therefore, to define the boundaries of each membership function we need 13 genes for the error and difference error variables and 16 genes for the actuation variable, as shown in Fig. 10.

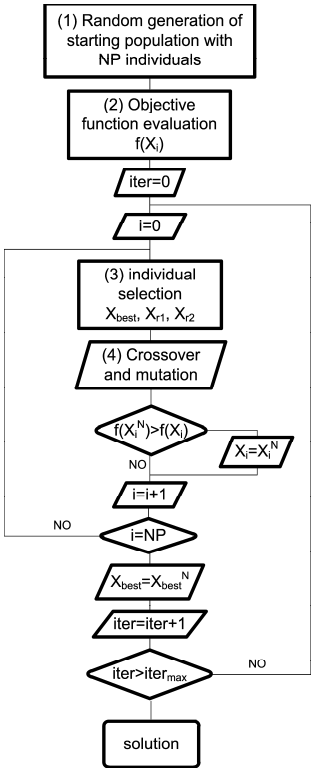

Fig. 9. Genetic algortihm

Two genes of the group of genes define the rank of each variable, the smallest and the highest, and the rest are sorted between these limits from the lowest to the highest, so the first gene represents the lower limit of the first membership function of each variable and the last gene represents the upper limit of the last membership function. The rest of the genes are the remaining boundaries of the membership functions (see Figure 10).

This method of defining membership functions guarantees that all the input and output variable values excite at least one membership function.

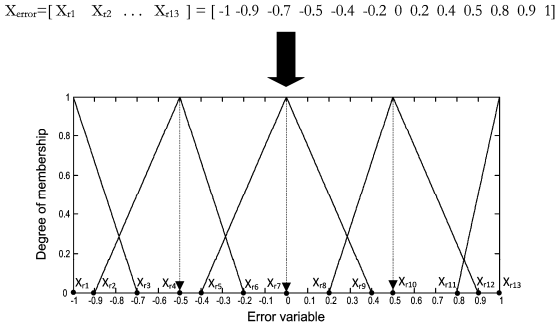

Fig. 10. Example of generated membership function

Once the initial population of *NP* individuals has been generated, it can be evolved to new populations in which its members produce a better solution to the problem. To perform this process, the evolutionary algorithm has to carry out the selection, reproduction, mutation and evaluation operations with the components of the population iteratively. These operations are implemented in a different way to the membership functions and rules.

The second step in our algorithm is the evaluation of the objective function. As explained above, each one of the elements of our population (chromosome) will be X_i, which represents a traction control block. The objective function is to maximize the distance travelled by the motorcycle in 2 seconds of simulation. The motorcycle model explained in section II is used to obtain the measurements needed by the control block and the travelled distances. Besides, we include the following equation which models the rear wheel:

$$J\dot{\omega}_r = T - Fx, r.R_r \tag{15}$$

Where J, ω_r and R_r are the inertial moment, angular velocity and radius of the rear wheel respectively. T is the driving torque, which is defined as:

$$T(t) = \left(1 - e^{-\frac{t}{Tc}}\right) \cdot K \cdot \eta \cdot Te(\omega_e, u(t), gear) \tag{16}$$

Where Tc is a time constant used to model the transient period while the engine is engaging. K is the transmission ratio, η is the efficiency of transmission and Te is the engine torque. The engine torque is obtained from the power curve of the motorbike as a function of engine revs (ω_e), throttle position, ($u(t)$), and gear engaged ($gear$). The scheme of the optimization process is shown in Fig. 11.

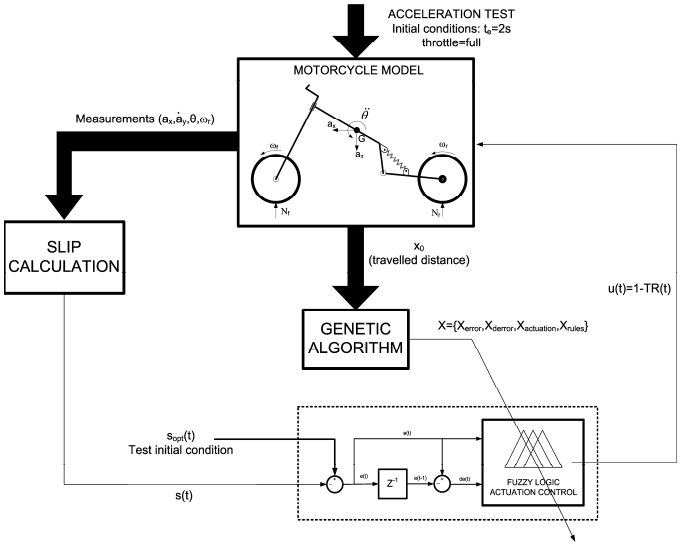

Fig. 11. Scheme of optimization process and evaluation of the objective function.

Once the fuzzy control has been optimized, more accurate simulations are carried out by a well-known dynamic motorcycle software called BikeSim®. The motorcycle model used by the Bikesim® software is fully documented in [24], with background material in [25]. Bikesim® software can be integrated in Simulink®, so we make use of the fuzzy logic toolbox of Simulink® and the flexibility of Matlab® to program the control algorithm. The objective function is shown in equation (21), where the *distance* function calculates the distance travelled by the motorcycle through the motorcycle model.

$$f_{obj}(X) = \max\{distance(X)\} \tag{21}$$

The third step is individual selection for reproduction. In this work we use a scheme known as differential evolution [26]. In this scheme, the selection of individuals for reproduction is carried out as follows: one of the parents is the i individual of the current population (X_i). To generate the other parent, called V parent, the best member of the current population (X_{best}) and two randomly chosen members (X_{r1} and X_{r2}) are selected and combined according to equation (22). Where F measures the deviation from the best member.

$$V = X_{best} + F(X_{r1} - X_{r2}) \tag{22}$$

The following step in the algorithm is crossover and mutation. In the crossover operator, the two parents (X_i and V) chosen for reproduction generate a new offspring (X_i^N). In the crossover process, genes of parents X_i and V are interchanged with a CP probability (Fig. 12).

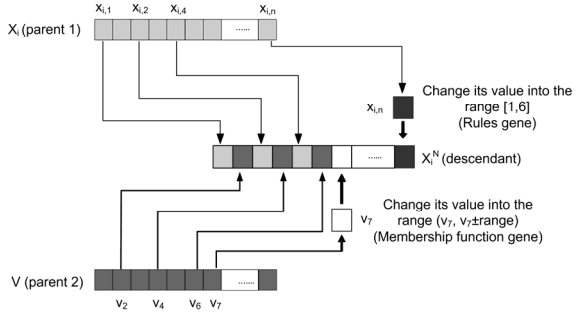

Fig. 12. Crossover and mutation operator.

Simultaneously with reproduction, operator mutation is carried out. Mutation is an operator consisting of random change of a gene during reproduction. In the original differential evolution algorithm [26], the mutation operator was not introduced.

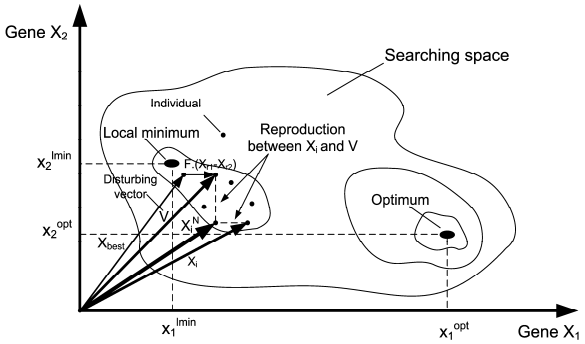

Fig. 13. Differential Evolution without mutation procedure.

A new mutation procedure of the parameters to be optimized is developed in this work. We have verified that this procedure is fundamental to obtain the optimum when the parameter range values are very different. The mutation

procedure changes only some of these parameters allowing to find the correct optimum and not to stop in a local minimum.

This problem was called stagnation in the work performed by Lampinen [27] and it is shown in Fig. 13.

The whole procedure to obtain a new descendent in the original differential evolution algorithm is shown in Fig. 13. In this case, there are two different parameters (genes) and the optimum has a very different value for these two parameters. As you can see in Fig. 13, to obtain the new descendant, X_i^N, the reproduction operator takes gene x_1 from parent V and x_2 form X_i. The new descendant seems to be worse than X_i because there is more distance to the global optimum, but the algorithm does not reject it because it has a better value of the objective function as it is closer to a local minimum. In this case, the V and X_i couple generates the X_i^N descendent, but this new chromosome may not reach the global minimum due to the fact that the absolute values of the genes that compose it are very different, and the selection plus reproduction operations are not able to make the new descendent by themselves to overcome the valley of the local minimum.

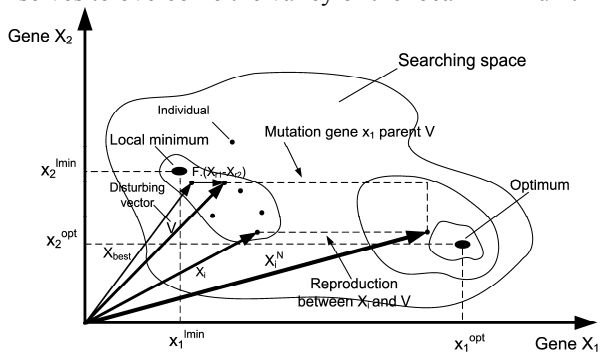

Fig. 14. Differential Evolution with mutation procedure.

With the mutation procedure, it is possible to solve the problem explained before. The generation of a new descendant using the mutation procedure is schemed in Fig. 14. Here, the value of one or several of the genes of the V and X_i couple is changed in a range defined by the user when reproduction is taking place. This fact yields a new descendent, X_i^N, which has a different fitness from the X_i^N descendent studied in the previous case. This allows the algorithm to look for individuals with better fitness in the next generation. In this work, mutation is defined as follows: depending on the mutation probability, genes of each parent can be chosen to mutate, for example if, gene $x_{i,n}$ mutates and belongs to the membership function genes ($n \in [1, 42]$), the operator randomly chooses a value within the interval of real values ($x_{i,n}$, $x_{i,n}$±*range*), which is added to or subtracted from $x_{i,n}$, depending on the direction of the mutation. But, if gene $x_{i,n}$ belongs to rule genes ($n \in [43, 67]$), then the operator randomly chooses a integer value between 1 to 6. Mutation is carried out with a probability defined as $MP \in [0, 1]$, much lower than *CP*. How the reproduction and mutation operator works is shown in Fig. 12.

Therefore, when the operations have been fulfilled, we have a new element, X_i^N. This new individual could substitute its parent, X_i, i.e., if, after crossover and mutation, the descendant (X_i^N) is better than X_i, the descendant substitutes the parent in the new population. Consequently, the new population neither increases nor decreases.

$$f(X_i^N) > f(X_i) \Longrightarrow X_i = X_i^N \tag{23}$$

Once the optimization algorithm has been described, in the next section we obtain an optimized traction control block in different acceleration tests and compare the results with the traction control based on experience and with the motorcycle without traction control.

V. Optimization Results

Optimizations and simulations have been carried out using different surfaces BikeSim® defines the surfaces with a parameter related to its adherence. For a better comprehension and interpretation, Fig. 15 shows the approximated adherence curves as a function of the longitudinal slip for different values of this parameter. These curves are approximate since real adherence depends, among other factors, on speed, slip angle or type of tire.

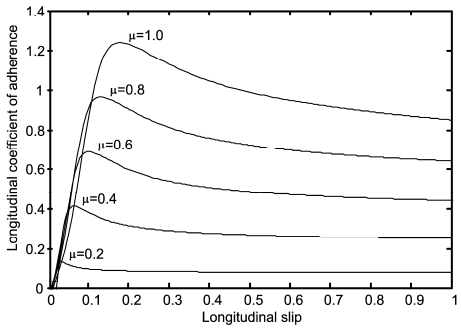

Fig. 15. Longitudinal adhesion curves in BikeSim®

The first fuzzy control has been optimized for a very slippery surface, defined as a $\mu = 0{,}4$ road. For this case, the programmed acceleration test used has the following initial conditions: The motorcycle model used is a sport racing-style bike with chain drive. The more relevant geometric parameter values can be found in Appendix B. Simulation parameters are the following: initial motorcycle velocity, $v_x(0)$=0 m/s, full throttle during the whole test, the clutch is completely engaged after 0.1 s. and simulation time, t_s=2 seconds. The simulation time is established this way because simulations are time-consuming and the slip between wheel and road is higher in initial instants. The objective of the optimized traction control is carrying out appropriate throttle reductions to obtain the maximum travelled distance. The parameters of the genetic algorithm are: individuals in the population *NP*=20, crossover probability *CP*=0.4, mutation probability *MP*=0.1, perturbation parameter *F*=0.6 and number of iterations *iter*=1000.

The travelled distance evolution of the best individual is shown in Fig. 16. As observed, the objective function evolves very fast in the first 500 iterations and more smoothly in the following iterations. The maximum distance reached is 5.126 meters after 2 seconds of the simulation.

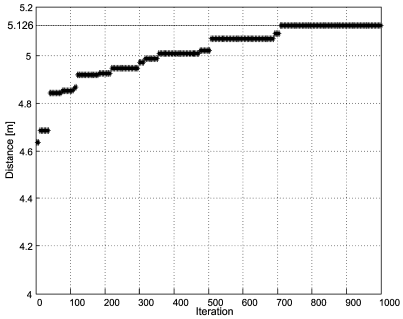

Fig. 16. Iterative process for optimization for road μ=0.4

The optimized membership functions of the output and input variables are shown in Fig. 17. The optimization algorithm has no constraint to determine the boundaries of input and output variables, but as we can see in Fig. 17, the limits of the variables are very similar to the control based on experience.

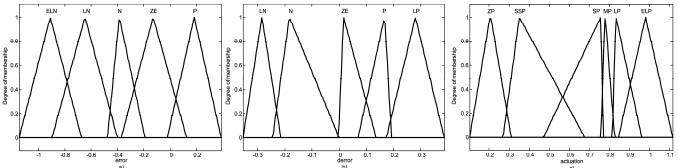

Fig. 17. Optimized membership functions for a μ=0.4 road. (a) Error input. (b) Derror input. (c) Actuation output

Finally the rules are shown in Table III. In this case, the number of existing rules is 18, which is lower than in the control based on experience. The control surface is shown in Fig. 18.

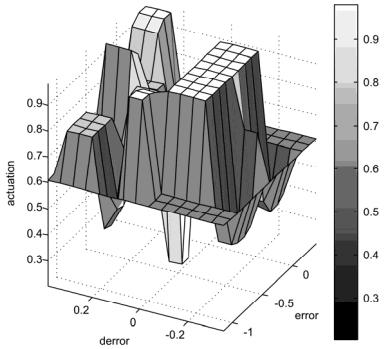

Fig. 18. Actuation surface for road μ=0.4

TABLE III
OPTIMIZED RULES FOR ROAD μ =0.4

error \ diferror	*LN*	*N*	*ZE*	*P*	*LP*
ELN			ELP	SSP	MP
LN	SSP	ELP	LP	LP	
N	MP	ELP	ZP	MP	ELP
ZE	SSP	ELP			MP
P			SP	SP	ELP

To compare the performance of the optimized control, we carry out the same acceleration test in μ=0.4 and μ=0.6 roads. The results are shown in Fig. 19. As expected, the optimized control is significantly better than the control based on experience and the motorcycle without traction control when the road is μ=0.4 (Fig. 19a), but when the road is μ=0.6, a slippery road, the control based on experience is the best control and the optimized control does not work efficiently (Fig. 19b). This is because the optimized control has been trained only for μ=0.4 roads and it is specialized in this kind of surface, reducing its performance when tested on other roads.

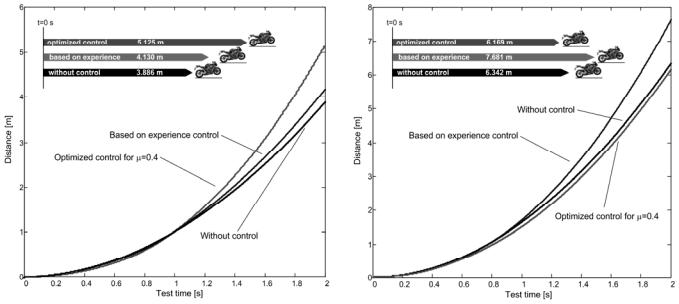

Fig. 19. (a) Optimized control for a μ =0.4 road running on a μ =0.4 road. (b) Optimized control for a μ =0.4 road running on a μ =0.6 road.

The same conclusion that we reached in the previous test happens when the control is optimized only on a μ=0.6 road (see Fig. 20). Again, the optimized control has the best result on the μ=0.6 road (Fig. 20a), but it loses efficiency when tested on other surfaces not included in the training (Fig. 20b). To solve this problem, we have to train our control on different surfaces or roads. Therefore, we carry out a new acceleration test which has the same initial conditions as in the previous example. In this case, the acceleration test is 2 seconds for both roads and the travelled distance evolution of the best individual, which is shown in Fig. 21, is the sum of the obtained distance for μ_1=0.4 and μ_2=0.6 roads. The parameters of the algorithm are in this case: number of individuals in the population *NP*=20, crossover probability *CP*=0.4, mutation probability *MP*=0.1, perturbation parameter *F*=0.6 and number of iterations *iter*=1000.

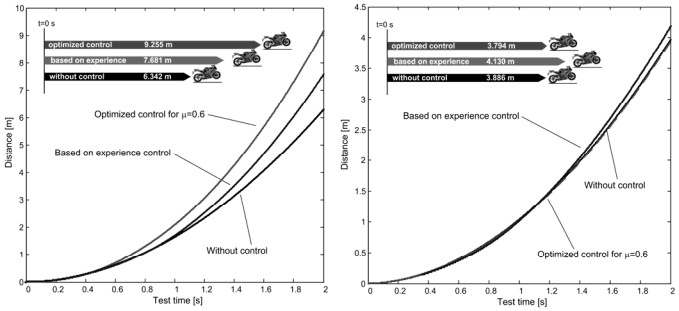

Fig. 20. (a) Optimized control for a μ =0.6 road running on a μ =0.6 road. (b) Optimized control for a μ =0.6 road running on a μ =0.4 road.

In this case, the travelled distance of the best individual evolves continuously and the maximum distance is reached in 4.780 meters for μ=0.4 roads and 8.429 meters for μ=0.6 roads. These values are slightly lower than those obtained in the previous cases, but very close to them.

In this case, the optimized membership functions of the output and input variables are shown in Fig. 21. Again, the

boundaries of input and output variables are very close to the limits of variables based on experience.

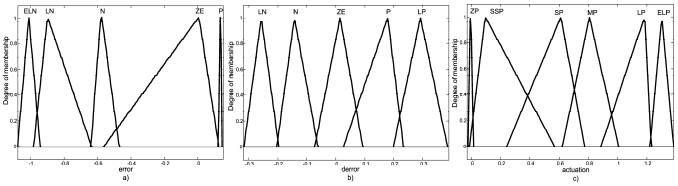

Fig. 21. Membership functions for mixed optimization. (a) Error input. (b) Derror input. (c) Actuation output.

The control surface is shown in Fig. 22 and the rules in Table IV. The number of rules is 19.

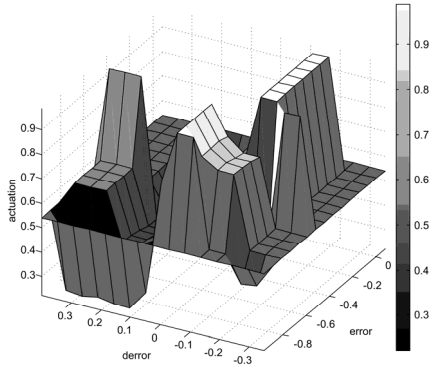

Fig. 22. Actuation surface: road μ_1=0.4 and μ_2=0.6

TABLE IV
TWO ANTECEDENT RULES: $\mu_1 = 0.4$ AND $\mu_2 = 0.6$

error \ diferror	***LN***	***N***	***ZE***	***P***	***LP***
ELN	SP		ELP	SSP	SSP
LN		LP	ELP	SP	MP
N	ELP	SP			ELP
ZE		ELP	MP	SP	
P	SSP	ZP	SSP	ELP	SP

A comparison of the performance of the mixed optimized control against the control based on experience and the motorcycle without traction control on both roads is shown in Fig. 23.

In Fig. 23a and 23c, the test was done on a μ=0.4 road. In this case, the travelled distance and the motorcycle speed obtained by mixed optimized control is significantly better than those achieved by control based on experience and the motorcycle without traction control. Concretely, mixed optimized control improves the travelled distance by 15.7% and vehicle velocity by 28.3% from the results reached by the control based on experience and the travelled distance by 23% and the velocity by 40.6% from the results obtained by the motorcycle without control. If the test is carried out on a μ=0.6 road (Fig. 23b and 23d), again the mixed optimized control is the best control. In this case, the optimized control improves the travelled distance by 9.7% and velocity by 6.7% from those obtained by control based on experience and the travelled distance by 32.9% and velocity by 42.2% from those achieved by the motorcycle without control. Therefore, this control works appropriately in both cases.

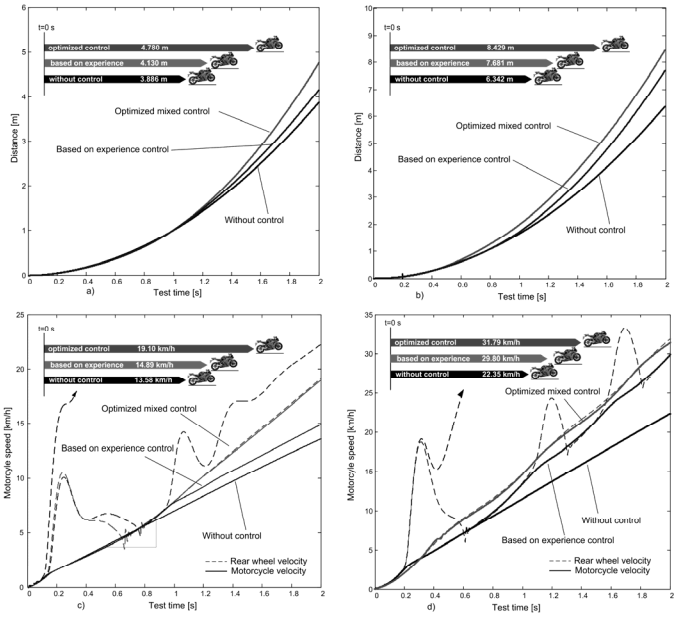

Fig. 23. (a) Travelled distance comparison on a μ=0.4 road. (b) Travelled distance comparison on a μ=0.6 road. (c) Motorcycle velocity comparison on a μ=0.4 road. (d) Motorcycle velocity comparison on a μ=0.6 road.

The rear wheel velocity is included in the previous figures (Fig. 23c and 23d). Without control, the rear wheel speed quickly increases causing a high wheel slippage during the whole test. When using the based on experience or the optimized control, the wheel speed is regulated, avoiding high slip and working close to the optimal slip zone.

Simulations using different surfaces have been carried out. Simulation parameters are the following: initial motorcycle velocity, $v_x(0)$=1.39 m/s, full throttle during the whole test, the clutch is completely engaged after 0.1 s. and simulation time, t_s=2 seconds. As seen in Table V, mixed optimized control achieves the highest travelled distances under low adherence conditions. Without control the distances are always smaller except for the surface defined as μ=0.8. This is due to fact that, on that surface, adherence is high and therefore the slip of the wheel is small during the test, so the control does not have to actuate.

TABLE V
TRAVELLED DISTANCE ON DIFFERENT SURFACES

	μ=0.2	**μ=0.4**	**μ=0.6**	**μ=0.8**
Mixed optimized control	5.026 m	7.047 m	11.501 m	13.057 m
Based on experience	4.592 m	6.821 m	10.601 m	13.057 m
Without control	4.588 m	6.587 m	8.987 m	13.057 m

Once the optimized control has been tested in straight-line traction on different surfaces, we subject our control to different tests to verify its adaptation to different maneuvers and simulations. In the first place, a test where the motorcycle carries out a sudden change of trajectory is realized. The initial conditions of this test are the following: initial motorcycle velocity $v_x(0)$=0 m/s, full throttle during the whole test. After running straight-lined for 0.5 seconds, a pulse of 2 Nm is applied to the handlebar. This pulse lasts 0.1 seconds and the motorcycle continues in a straight line afterwards. The

simulation time in this test is t_s=6 seconds and the road is μ=0.4.

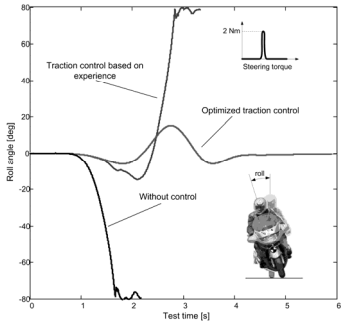

Fig. 24. Motorcycle roll angle when a sudden event is applied.

The result of this test is shown in Fig. 24. In this figure the roll angle of the motorcycle is drawn. The optimized control is able to get over the sudden torque and the motorcycle continues until the end of the test, but the motorcycle without control and with a control based on experience falls down and cannot continue. This test simulates an unexpected event, which is common when a rider wants to avoid some kind of obstacle or a pothole pushes the motorcycle laterally. The optimized control maintains the stability avoiding falling on the ground.

On the other hand, a new test where the rider tries to perform a trajectory curve on a slippery road is carried out. In this test, the initial motorcycle velocity is $v_x(0)$=0 m/s and full throttle during the whole test. After 0.5 seconds in a straight line, a lean angle of 20º is imposed. This lean angle provokes the motorcycle to carry out a curve. The simulation time in this test is t_s=6 seconds and the road is μ=0.6. The roll angle of the motorcycle is shown in Fig. 25a. The motorcycle without control cannot avoid losing control and falling on the road just because the throttle is full when we impose a very hard lean angle on the motorcycle. The same happens when the traction control based on experience tries to control the throttle. As its action is not sufficient, the motorcycle loses control as well. But the optimized traction control is able to avoid losing control and maintain the motorcycle in an appropriate trajectory (Fig. 25b)

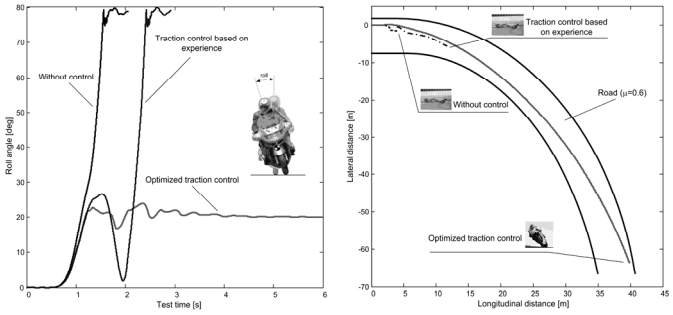

Fig. 25. (a) Roll angle in the lean angle test. (b) Motorcycle trajectory

As demonstrated, the mixed fuzzy control is a good selection if the motorcycle has to be prepared for different surfaces or road types. We have seen that the optimized mixed fuzzy control is a good choice to improve safety and performance in a motorcycle. However, another option is using different optimized fuzzy controls for different road types making the traction control choose the appropriate optimized fuzzy control in each moment. This is possible because the traction control can detect the road type the motorcycle is riding on.

To compare our control, we carried out test described in [2]. The authors called this test a μ-jump, where initial motorcycle velocity was $v_x(0)$=14.1 m/s, with full throttle during the whole test. After running straight-lined for 6.15 seconds on a μ=0.2 surface, we changed to a μ=0.4 surface and the test finished at 10 seconds. Fig. 26 shows that our proposed control can guarantee safety also in very critical maneuvers. As we can see, our control maintains the slip very close to the optimum and reaction time is faster than in the simulation shown in [2]. For this reason vehicle speed at the end of the test is better with our control.

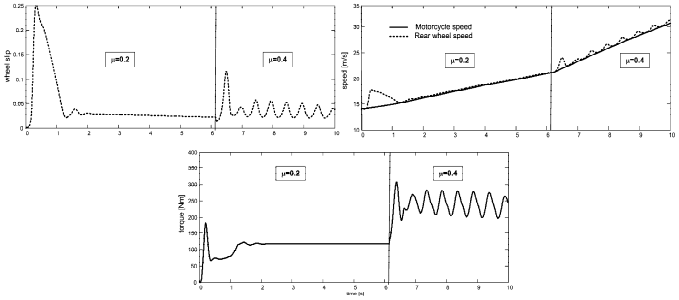

Fig. 26. (Top - left) Relative rear wheel slip. (Top - right) (solid line) vehicle speed and (dashed line) rear wheel speed. (Bottom) Driving torque (u(t)=1-TR(t)).

VI. CONCLUSION

In this work, a novel motorcycle traction control has been described. The new system improves safety and facilitates handling since it can prevent the rear wheel from slipping and the lack of control associated with it.

TCS have hardly been applied to street or racing motorcycles. When strong accelerations or adherence reduction occurs, the-lack-of-traction problem appears and the dynamics of the motorcycle is strongly affected. One of the principal consequences is that the slip in the rear wheel increases, causing a reduction in acceleration capacity of the motorbike or reducing vehicle stability. This fact makes it convenient to develop a system to enhance vehicle control under such circumstances, that is, when the slip takes values above the optimum.

The proposed control block is based on the use of fuzzy logic. The inputs to the control block are the actual slip in the rear wheel, which is estimated using an Extended Kalman Filter, and the optimal slip, which is obtained by means of a neural network.

Four fuzzy inference engines have been used. The first one is fitted using expert knowledge of slip evolution in traction processes. The remaining three have been optimized by using an evolutionary algorithm based on differential evolution. The optimization algorithm has been used to automatically generate optimal control blocks for two surfaces separately and for both surfaces together. The optimized control blocks

improve the results obtained with the one based on expert knowledge. This makes it possible to select a control block optimized for one single surface or a generic control optimized for several surfaces.

The control blocks have been tested using BikeSim®. Simulations on two different surfaces and in mixed conditions have been carried out. The test includes the results obtained with the optimized fuzzy TCS and without TCS. Both fuzzy logics based T.C.S. produce significant improvements, maintaining the slip within the optimal region and with few oscillations in the slip compared to the motorcycle without control. The best results are obtained with the optimized control blocks, which improve distance and stability considerably compared to the based-on-experience controller and with the motorcycle without TCS. Further work on TCS systems combining braking and injection system controls are being developed at the moment.

APPENDIX A

An important fact in vehicle control systems is to determine its stability and robustness. The stability of the fuzzy control based on experience was studied in section III. In this appendix, the performance of the controllers (based on experience and optimized) has been verified using cell mapping [28-30]. The state space has been partitioned into 30x20 cells. Stability, robustness and efficiency are evaluated for any possible initial error and derror variable values. An acceleration test on a low adherence surface has been employed for the evaluation. Stability and distance covered during the first three seconds of simulation are taken into account.

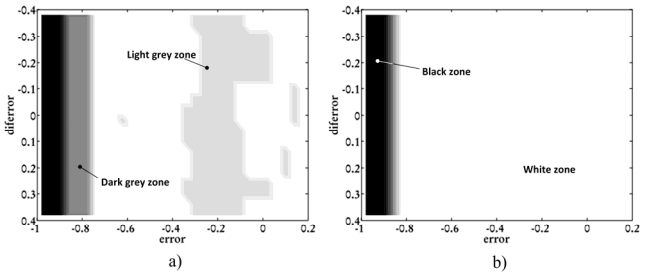

Fig. 27. Cell mapping corresponding to the following control: (a) Optimized. (b)Based-on-experience.

Figure 27 shows the result of the evaluation. According to the error definition and considering optimal slip for this surface, 0.12, the error cannot take values below -0.88. This is reproduced in the figure with a black zone. Dark grey zones are cells whose efficiency are not satisfactory, that is, the distance reached is well below optimal distance or full wheel slip is reached during the simulation. Equilibrium is achieved if the control is able to stabilize the error and diferror within the cells surrounding the zero error and diferror point. Light grey zones are cells that reach a stable condition but not within the equilibrium region. Finally, white zones indicate stable cells. The first image is the cell mapping corresponding to the control in which functions and rules were optimized using genetic algorithms and the second image is obtained with the control that is based on experience. Both systems are stable because the controls are always capable of ending in a stable condition. However, the optimized control does not always reach the equilibrium region, as seen in Figure 27-a.

APPENDIX B

TABLE VI
MOTORCYCLE PROPERTIES

Motorcycle geometric and mechanical properties.		**Rear suspension properties**	
Wheelbase	1.370 m	Spring stiffness	40,000 N/m
Center of mass height (vehicle with rider)	0.621 m	Spring pre-load	1182 N
Center of mass distance from front wheel	0.560 m	Spring travel	0.2 m
Caster angle	27.72º	Damping coefficient	10,000 Ns/m
Rear arm length	0.426 m	Swing arm mass	8 kg
Mass of vehicle with rider	274.6 kg	**Front suspension properties**	
Front wheel mass	12.7 kg	Spring stiffness	25,000 N/m
Rear wheel mass	14.7 kg	Spring pre-load	933 N
Frame pitch inertia	22 kgm^2	Spring travel	0.12 m
Front wheel moment of inertia	0.484 kgm^2	Damping coefficient	2000 Ns/m7
Rear wheel moment of inertia	0.638 kgm^2	Front fork mass	7.25 kg
Frontal cross section area	0.6 m^2	**Tire properties**	
Drag coefficient	0.52	Radial stiffness of front tire	130,000 N/m
Lift coefficient	0.085	Radial stiffness of rear tire	141,000 N/m
Pitch coefficient	0.205	**Engine properties**	
		Opening throttle time constant	0.15 s
		Closing throttle time constant	0.15 s

REFERENCES

[1] M. Corno, S. Savaresi, M. Tanelli and L. Fabbri, “On optimal motorcycle braking”, Control Engineering Practice, vol. 16, no. 6, pp. 644-657, Jun. 2008.

[2] M. Tanelli, C. Vecchio, M. Corno, A. Ferrara and S. Savaresi, “Traction Control for Ride-by-Wire Sport Motorcycles: A Second-Order Sliding Mode Approach”, IEEE Transactions on Industrial Electronics, vol. 56, no. 9, pp. 3347-3356, Sep. 2009.

[3] P. Cardinale, C. D'Angelo and M. A Conti, “Traction Control System for Motocross and Supermotard”, presented at the International Workshop on Intelligent Solutions in Embedded Systems, Regensburg, Jul. 10-11, 2008.

[4] C. Bo-Chiuan, C. Chia-Hsing and H. Shiuh-Jer, “Fuzzy Sliding Mode Control of Traction Control System for Electric Scooter”, presented at the Seventh International Conference on Fuzzy Systems and Knowledge Discovery, Yantai, Shandong, Aug. 10-12, 2010.

[5] M. Massaro, R. Sartori and R. Lot, “Numerical investigation of engine-to-slip dynamics for motorcycle traction control applications”, Vehicle System Dynamics, vol. 43, no. 3, pp. 419-432, Mar. 2011.

[6] M. Shin, J. Han, J. Youn and M. Sunwoo, “Design of a Networked Traction Control System using a Real-Time Operating System”, in Proc. of the IMechE, Part D: Journal of Automobile Engineering vol. 222, pp. 1395-1408, Aug. 2008.

[7] M. Corno, S. Savaresi and G. Balas, “Linear, Parameter-Varying Wheel Slip Control for Two-Wheeled Vehicles”, in Proc. of the 47th IEEE Conference on Decision and Control, Cancun, Mexico, 2008.

[8] T. Wakabayashe, T. Matsuto, K. Tani and A. Ohta, “Development of motor actuated antilock brake system for light weight motorcycle”, JSAE review, vol. 19, no. 4, pp. 373-377, Oct. 1998.

[9] R. J. Miennert, “Antilock Brake System Application to a Motorcycle Front Wheel”, *SAE Preprints,* vol. n 740630, 1974.

[10] V.D. Colli, G. Tomassi and M. Scarano, “Single Wheel’ Longitudinal Traction Control for Electric Vehicles”, IEEE Transactions on Power Electronics, vol. 21, no. 3, pp. 799-808, May 2006.

[11] J.A. Cabrera, A. Ortiz, J.J. Castillo and A. Simón, “A Fuzzy logic control for antilock braking system integrated in IMMa tire test bench”, IEEE Transactions on Vehicular Technology, vol. 54, no. 6, pp. 1937-1949, Nov. 2005.

[12] G.F. Mauer, “A Fuzzy Logic Controller for an ABS Braking System”, IEEE Transactions on Fuzzy Systems, vol. 3, no. 4, pp.381-388, Nov. 1995.

[13] M.V.C. Rao and V. A. Prahlad, “Tunable fuzzy logic controller for vehicle-active suspension systems”, Fuzzy Sets and Systems, vol. 85, no. 1, pp. 11-21, Jan. 1997.

[14] H. Du and N. Zhang, "Fuzzy Control for Nonlinear Uncertain Electrohydraulic Active Suspensions with Input Constraint", IEEE Transactions on Fuzzy Systems, vol. 17, no. 2, pp. 343-356, Apr. 2009.
[15] L. Austin and D. Morrey, "Recent Advances in Antilock Braking Systems and Traction Control Systems" in Proc. of the IMechE, Part D: Journal of Automobile Engineering, vol. 214, pp. 625-638, Jun. 2000.
[16] O. Cordon, F. Gormide, F. Herrera, F. Hoffmann and L. Magdalena, "Ten years of genetic fuzzy systems: current framework and new trends", Fuzzy Sets and Systems, vol. 141, no.1, pp. 5-31, Jan. 2004.
[17] Y.C. Chiou and L.W. Lan, "Genetic fuzzy logic controller: an iterative evolution algorithm with new encoding method", Fuzzy Sets and Systems, vol. 152, no. 3, pp. 617-635, Jun. 2005.
[18] F. Cheong and R. Lai, "Designing a hierarchical fuzzy logic controller using the differential evolution approach", Applied Soft Computing, vol. 7, no. 2, pp. 481-491, Mar. 2007.
[19] H. B. Pacejka, *Tyre and vehicle dynamics*, Oxford: Elsevier Ltd., 2006.
[20] M. Burckhardt, *Fahrnverktechnik: Radschlupfregelsysteme*, Germany: Vogel-Verlag, 1993.
[21] L. Ray, "Nonlinear Tire Force Estimation and Road Friction Identification: Simulation and Experiments", Automatica, vol. 33, no. 10, pp. 1819-1833, Oct. 1997.
[22] W. Pedrycz, *Fuzzy Control and Fuzzy Systems*, New York: Wiley, 1989.
[23] H.J. Zimmermann, *Fuzzy Set Theory and its Applications*, London: Kluwer Academic Publishers, 1985.
[24] R.S. Sharp, S. Evangelou and D.J.N. Limebeer, "Advances in the Modelling of Motorcycle Dynamics", Multibody System Dynamics, vol. 12, no.3, pp. 251-283, Oct. 2004.
[25] R.S. Sharp and D.J.N. Limebeer, "A Motorcycle Model for Stability and Control Analysis", Multibody System Dynamics", vol. 6, no. 2, pp. 123-142, Sep. 2001.
[26] R. Storn and K. Price, "Differential Evolution. A Simple and Efficient Heuristic Scheme for Global Optimization over Continuous Spaces", Journal of Global Optim., vol. 11, no.4, pp. 341-359, Dec. 1997.
[27] J. Lampinen and I. Zelinka, "On Stagnation of the Differential Evolution Algorithm", in Proc. of MENDEL 2000, Brno, Czech, 2000, pp. 76-83.
[28] J. Fei and C. Isik,"The analysis of fuzzy knowledge-based systems using cell-to-cell mapping", in Proc. of the 5th IEEE International Symposium on Intelligent Control, Philadelphia, PA., pp.633,637 vol.1, 5-7 Sep 1990.
[29] J Levitas, "Global stability analysis of fuzzy controllers using cell mapping methods", Fuzzy Sets and Systems, vol 106, no. 1, pp. 85-97, Aug. 1999.
[30] M. Papa, J. Wood and S. Shenoi, "Evaluating controller robustness using cell mapping", Fuzzy Sets and Systems, vol. 121, no. 1, pp.3-12, Jul. 2001.

Juan A. Cabrera received the B.S. in mechanical engineering, M.S. in computer science, and Ph.D. degrees in mechanical engineering from the University of Malaga, Spain.
He is an Associate Professor of Mechanical Engineering at the University of Malaga. His research interests include modeling and control of vehicle systems, advanced vehicle systems, genetic algorithms applied to mechanisms and tire models, and multiobjective evolutionary strategies.

Juan J. Castillo received the B.S., M.S., and Ph.D. degrees in mechanical engineering from the University of Malaga, Spain.
He is an Associate Professor of Mechanical Engineering at the University of Malaga. His research interests include vehicle dynamics, modeling and control of vehicle safety systems and parameters estimation.

Enrique Carabias received the B.S. and M.S. from the Polytechnic University of Madrid, Spain, and is currently pursuing the Ph.D. degree in mechanical engineering from the University of Malaga, Spain.
He is an Assistant Professor of Mechanical Engineering at the University of Malaga. His research interests include vehicle dynamics, modeling and control of vehicle safety systems and parameters estimation.

Antonio Ortiz received the B.S. and M.S. degrees in mechanical engineering from the Polytechnic University of Madrid, Spain. He obtained his Ph.D. at the University of Malaga.
He is currently an Associate Professor of Mechanical Engineering at the University of Malaga.
His research interests include tire models, genetic algorithms and multiobjective evolutionary strategies. He also works over mechanisms and machines design.